Structural basis for the ethanol action on G-protein–activated inwardly rectifying potassium channel 1 revealed by NMR spectroscopy

Yuki Toyama[a,b], Hanaho Kano[a], Yoko Mase[a], Mariko Yokogawa[a,1], Masanori Osawa[a,1], and Ichio Shimada[a,2]

[a]Graduate School of Pharmaceutical Sciences, The University of Tokyo, Hongo, 113-0033 Tokyo, Japan; and [b]Japan Biological Informatics Consortium, Aomi, 135-0064 Tokyo, Japan

Edited by Gerhard Wagner, Harvard Medical School, Boston, MA, and approved March 2, 2018 (received for review December 21, 2017)

Ethanol consumption leads to a wide range of pharmacological effects by acting on the signaling proteins in the human nervous system, such as ion channels. Despite its familiarity and biological importance, very little is known about the molecular mechanisms underlying the ethanol action, due to extremely weak binding affinity and the dynamic nature of the ethanol interaction. In this research, we focused on the primary in vivo target of ethanol, G-protein–activated inwardly rectifying potassium channel (GIRK), which is responsible for the ethanol-induced analgesia. By utilizing solution NMR spectroscopy, we characterized the changes in the structure and dynamics of GIRK induced by ethanol binding. We demonstrated here that ethanol binds to GIRK with an apparent dissociation constant of 1.0 M and that the actual physiological binding site of ethanol is located on the cavity formed between the neighboring cytoplasmic regions of the GIRK tetramer. From the methyl-based NMR relaxation analyses, we revealed that ethanol activates GIRK by shifting the conformational equilibrium processes, which are responsible for the gating of GIRK, to stabilize an open conformation of the cytoplasmic ion gate. We suggest that the dynamic molecular mechanism of the ethanol-induced activation of GIRK represents a general model of the ethanol action on signaling proteins in the human nervous system.

NMR | GIRK | ethanol | ion channels

Ethanol exerts a wide range of physiological effects, such as cognitive-impairing, anxiolytic, and analgesic effects, by modulating the activities of various types of signaling proteins in the central nervous system, particularly ion channels (1, 2). Although numerous target proteins of ethanol have been identified so far, the detailed molecular mechanisms underlying the ethanol action have still remained unclear. Structural and biochemical analyses would facilitate the development of anesthetics and other pharmaceutical compounds acting on the central nervous system, since it has been proposed that ethanol and anesthetics produce similar pharmacological effects by binding to an overlapping site (3–5). The ion channels associated with the ethanol action include *N*-methyl-D-aspartate receptors (6), γ-amino butyric acid receptors (7), and G-protein–activated inwardly rectifying potassium channels (GIRK) (8–10). GIRK is a member of the inwardly rectifying potassium channel (Kir) family, which regulates neural excitabilities (11, 12). Along with the βγ subunit of G protein (Gβγ) released upon the activation of G-protein–coupled receptors, ethanol is known to directly open GIRK. The opening of GIRK is invoked by ethanol at physiologically relevant concentrations (on the order of 10^{-2} M, or 0.1% blood alcohol level), and behavioral studies have shown that weaver mutant mice, which have mutated GIRK with impaired K^+ selectivity, and GIRK knockout mice exhibited diminished ethanol-induced analgesia (8, 10, 13–15). These observations indicate that the opening of GIRK by ethanol is closely related to the ethanol action in vivo.

GIRK functions as a tetramer, consisting of a transmembrane (TM) and a cytoplasmic (CP) region, and a K^+ pathway is formed at the center of the tetramer. GIRK possesses two K^+ gates: the helix bundle crossing formed by the TM helices and the G-loop on the membrane side of the CP region (Fig. S1*A*) (16–19). Although the structure of GIRK bound to ethanol has not yet been solved, the crystal structure of a different subtype of Kir, Kir2.1, bound to an alcohol compound, 2-methyl-2,4-pentanediol (MPD), suggested that the alcohol binding pocket is located at the interface between the two neighboring cytoplasmic regions, and a similar cavity is also found in the corresponding position of GIRK (Fig. S1 *B* and *C*) (20, 21). Recently, Bodhinathan and Slesinger (22) revealed that ethanol binding involves an increase in the affinity for a membrane phosphatidylinositol 4,5-bisphosphate (PIP_2) by utilizing an alcohol-tagging strategy, in which a single thiol-reactive cysteine at or near the putative ethanol-binding pocket is chemically modified with a hydroxyethyl methanethiosulfonate reagent to mimic an ethanol-bound state. However, since these findings are based on results obtained using an alcohol with a different functional property (MPD actually inhibits Kir2.1), and chemical compounds covalently attached to GIRK, the actual functional ethanol-binding site of GIRK, the physiochemical properties of the interaction, and the structural changes induced by ethanol binding have still remained unclear.

One of the major difficulties in studying the mechanisms of the ethanol action is the extremely weak binding affinity, compared with typical protein–ligand interactions. Electrophysiological studies reported that the addition of 200 mM ethanol did not fully

Significance

Ethanol exerts various functions by acting on ion channels in neural systems. Despite its biological importance, molecular mechanisms underlying the ethanol action remained unknown, due to the weak binding affinity and the dynamic nature of the interaction. Here, by using solution NMR techniques, we investigated the molecular interaction of ethanol with G-protein–activated inwardly rectifying potassium channel (GIRK), which is a physiologically relevant target of ethanol, and revealed that ethanol activates GIRK by shifting the conformational equilibrium of GIRK to stabilize the open conformation of the cytoplasmic ion gate. These findings provide structural insights into mechanisms of the ethanol action for various types of ethanol-sensitive signaling molecules and would facilitate the developments of pharmaceutical compounds targeting ion channels.

Author contributions: Y.T., H.K., Y.M., M.Y., M.O., and I.S. designed research, performed research, analyzed data, and wrote the paper.

The authors declare no conflict of interest.

This article is a PNAS Direct Submission.

[1]Present address: Keio University Faculty of Pharmacy, 105-8512 Tokyo, Japan.

[2]To whom correspondence should be addressed. Email: shimada@iw-nmr.f.u-tokyo.ac.jp.

This article contains supporting information online at www.pnas.org/lookup/suppl/doi:10.1073/pnas.1722257115/-/DCSupplemental.

Published online March 26, 2018.

activate GIRK, suggesting that the binding affinity of ethanol is on the order of hundreds of millimolar or more (8, 9). The weak binding affinity of ethanol has also been reported for other ethanol-binding proteins and severely hampers the understanding of the nature of the ethanol binding and the detailed structural characterization of the ethanol-bound state (2). In fact, among the known ethanol-binding proteins, only a few structures of the specific ethanol–protein complexes have been solved so far (23, 24). Another roadblock is the dynamic nature of the ethanol action on proteins, which is usually difficult to characterize by conventional structural and biochemical methods. Solution NMR spectroscopy is one of the most powerful methods for studying the dynamic nature of proteins; however, the ethanol-binding proteins in the neural systems, such as ion channels, usually have large molecular weights over 100,000, thus hampering the applications of NMR. The ethanol-binding protein LUSH, an odorant binding protein from *Drosophila melanogaster*, has a relatively small molecular weight of 17,000 that is amenable to NMR analyses, and that revealed that ethanol binding induces few differences in the static structures and modulates conformational exchange processes of the proteins (23–25). Considering that the functional importance of conformational exchange processes has been proposed for various types of ion channels including GIRK (19, 26–28), the conformational exchange processes in GIRK and the ethanol action on them must be characterized to fully understand the mechanism of the ethanol action.

In this study, we investigated the ethanol action on GIRK by utilizing solution NMR techniques optimized for high–molecular-weight systems and analyzed the weak GIRK–ethanol interactions and conformational exchange processes of GIRK at atomic resolution. Our NMR analyses revealed that ethanol binds to the cavity formed between the neighboring cytoplasmic regions of GIRK, which is similar to the alcohol-binding pocket found in the Kir2.1–MPD complex, and induces structural and dynamic rearrangements of the cytoplasmic G-loop gate, with an apparent dissociation constant (K_d) of 1.0 M. Based on the results, we propose the dynamic activation mechanism of GIRK induced by ethanol.

Results

Chemical Shift Changes Observed in the GIRK CP Region upon Ethanol Addition. Electrophysiological studies using chimeric GIRK constructs revealed that the region responsible for the ethanol action is located in the CP region of GIRK (9). Therefore, we used the cytoplasmic regions of mouse GIRK1, composed of residues 41–63 and 190–371 fused into a single polypeptide ($GIRK_{CP}$) (16), to investigate the interaction with ethanol. The validity of the construct is supported by the facts that $GIRK_{CP}$ forms a tetrameric structure that is almost identical to the CP region in the full-length GIRK, and that $GIRK_{CP}$ can interact with physiological binding partners, such as polyamines, a Gβγ protein, and a Gα protein (17, 29–31).

To investigate the interaction of $GIRK_{CP}$ with ethanol, we analyzed the NMR spectral changes of $GIRK_{CP}$ upon the addition of ethanol. Although we previously reported the backbone amide ^{1}H–^{15}N resonance assignments, some residues forming the putative ethanol-binding pocket were not assigned, due to severe signal broadenings (32). To alleviate this problem, we adopted selective methyl-labeling strategies and applied methyl transverse relaxation-optimized spectroscopy (TROSY) techniques (33) that can be effectively applied to high–molecular-weight proteins, such as $GIRK_{CP}$ with a molecular weight of 96,000 as the tetramer. We prepared a {u-[^{2}H,^{15}N]; Alaβ, Ileδ1, Leuδ1, Valγ1, Metε-[$^{13}CH_3$]} $GIRK_{CP}$ sample, and analyzed the changes in the ^{1}H–^{13}C heteronuclear multiple quantum coherence (HMQC) spectra upon the addition of ethanol (Fig. 1*A* and Fig. S2). The overlaid ^{1}H–^{13}C HMQC spectra of $GIRK_{CP}$ in the presence (red) and absence (black) of 2.0 M ethanol are shown in Fig. 1*A*. Small but significant chemical shift changes were observed in some methyl groups upon the titration of ethanol (Fig. 1*B*). The apparent K_d of ethanol was calculated to be 1.0 M, by fitting the titration curves of the chemical shift changes to a theoretical formula assuming a simple bimolecular interaction between one ethanol molecule and one GIRK monomer (Fig. 1*C*). We conducted similar experiments using the L246W mutant, which showed decreased ethanol-mediated activation by perturbing the structure of the putative ethanol-binding pocket deduced from the Kir2.1–MPD structure (21), and confirmed that the observed chemical shift changes were not due to nonspecific interactions or changes in the solvation effects (*SI Text* and Fig. S3).

The methyl groups with chemical shift changes larger than 0.04 ppm were located on the βC strand (Val215), βE strand (Leu246), βF–βG loop (Leu264, Val265), βG strand (Ile270), βH strand (Val296, Ile298, Leu299, Ile302), βK–βL loop (Val330), βL strand (Leu333), and βM strand (Val340) (Fig. 1 *D* and *E*). Of these methyl groups, the methyl groups of Leu246 (βE) and Leu333 (βL strand) showed marked chemical shift changes larger than 0.09 ppm, which can be caused by the direct binding effect of ethanol. These methyl groups are clustered at the interface of the neighboring subunit and form a hydrophobic cavity on the solvent-exposed surface. These observations indicate that the cavity is responsible for the ethanol binding. Notably, Leu246 corresponds to Leu245 in Kir2.1 that forms the alcohol binding pocket identified in Kir2.1–MPD complex structure, strongly supporting the proposal that ethanol binds to the same pocket in GIRK as that identified in Kir2.1 (Fig. 1*E* and Fig. S1 *B* and *C*).

Conformational Exchange Processes of $GIRK_{CP}$ in the Absence of Ethanol. Although chemical shift changes were observed upon the addition of ethanol, they were smaller than 0.1 ppm for the majority of the methyl groups, suggesting that the static structure is not substantially perturbed by ethanol binding. Our recent NMR analyses of prokaryotic KirBac1.1, which shares high structural and functional similarities with the eukaryotic Kir (34, 35), revealed that the conformational exchange processes exist in the cytoplasmic region, where significant structural changes occur during gating (36). Thus, we investigated the possibility that ethanol activates GIRK by modulating the conformational exchange processes of $GIRK_{CP}$.

We conducted ^{1}H–^{13}C multiple-quantum (MQ) Carr–Purcell–Meiboom–Gill relaxation dispersion (CPMG RD) (37) and methyl–heteronuclear double resonance (HDR) (36) experiments, which can detect conformational exchange processes on millisecond-to-microsecond timescales, on the methyl groups of $GIRK_{CP}$ in the absence of ethanol. The plots of the exchange contributions to the MQ relaxation rates ($R_{MQ,ex}$), calculated using the effective MQ relaxation rates ($R_{MQ,eff}$) in the presence of 50 and 1,000 Hz CPMG pulse trains [$R_{MQ,ex} = R_{MQ,eff}$ (50 Hz) $- R_{MQ,eff}$ (1,000 Hz)], and the exchange contributions to the differential MQ relaxation rates ($\Delta R_{MQ,ex}$), are shown in Fig. 2*A*. We observed marked exchange contributions larger than 20 s^{-1} in some methyl groups, showing that conformational exchange processes on millisecond-to-microsecond timescales occur in $GIRK_{CP}$. Assuming a two-state exchange between the ground and excited states, we calculated the chemical shift changes ($\Delta\omega_C$ for ^{13}C, $\Delta\omega_H$ for ^{1}H), the exchange rate (k_{ex}), and the excited state population (p_E) for each methyl group, which could simultaneously explain the experimentally observed MQ CPMG RD curves and the $\Delta R_{MQ,ex}$ rates obtained from the methyl-HDR experiments (Fig. S4). The calculated k_{ex} and p_E values for Val215, Met223, Ile270, Ile298, Ala312, and Leu333 were almost identical, indicating that the two-state assumption holds for $GIRK_{CP}$ and the exchange process can be described by two distinct conformations exchanging in a cooperative manner. Thus, we globally analyzed the MQ CPMG RD curves and the

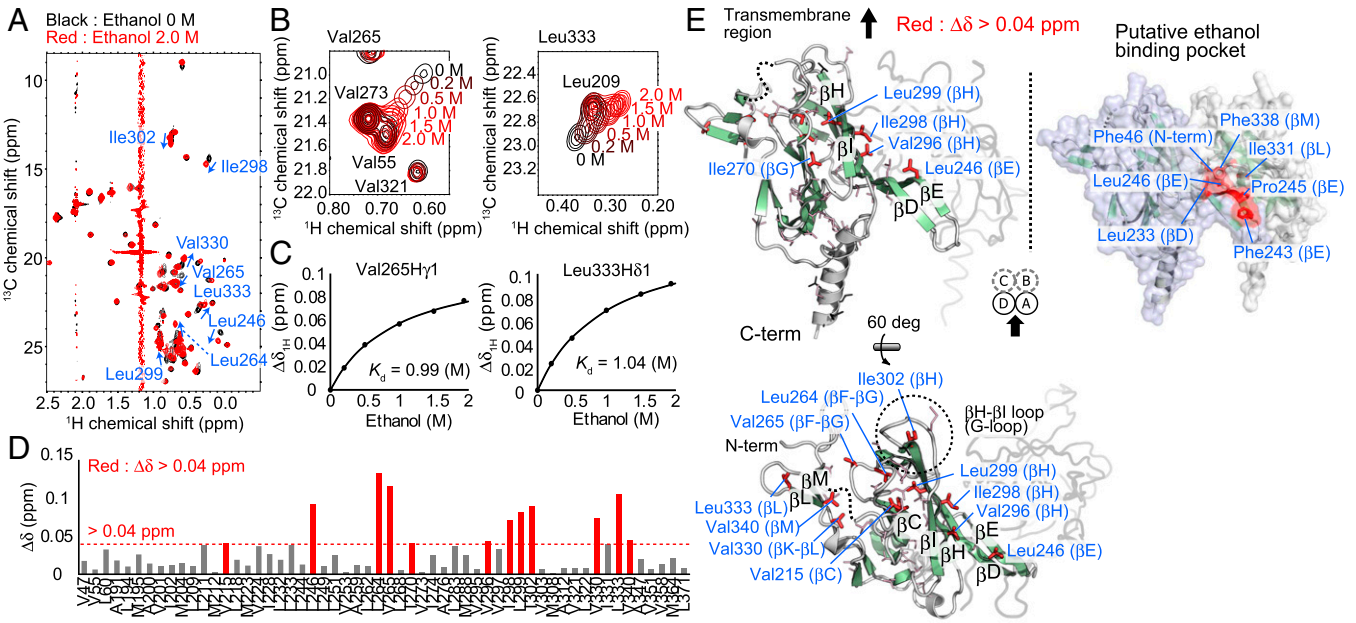

Fig. 1. NMR characterization of the interaction between $GIRK_{CP}$ and ethanol. (*A*) Overlay of the ^{1}H–^{13}C HMQC spectra of {u-[^{2}H, ^{15}N]; Alaβ, Ileδ1, Leuδ1, Valγ1, Metε-[$^{13}CH_3$]} $GIRK_{CP}$ in the presence (red) and absence (black) of 2.0 M ethanol. (*B*) The ethanol concentration-dependent chemical shift changes of Val265γ1 and Leu333δ1. (*C*) Plots of the ^{1}H chemical shift changes of Val265γ1 and Leu333δ1 as a function of the ethanol concentration. (*D*) Plots of the normalized chemical shift changes upon the addition of 2.0 M ethanol. The methyl groups with chemical shift changes larger than 0.04 ppm are colored red. The chemical shift changes, Δδ, are calculated by the equation, $\Delta\delta = \{(\Delta\delta_{1H})^2 + (\Delta\delta_{13C}/5.6)^2\}^{0.5}$. (*E*) Mapping of the methyl groups with marked chemical shift changes on the structure of $GIRK_{CP}$ (PDB ID code 1N9P) (16). The methyl groups with chemical shift differences larger than 0.04 ppm are shown as red sticks, and the other methyl groups are shown as stick models. The schematic drawing of the $GIRK_{CP}$ tetramer (subunits A, B, C, and D), viewed from the membrane side, is included to indicate the view of the mapping. The structure of the putative ethanol-binding pocket of $GIRK_{CP}$, deduced from the crystal structure of the Kir2.1–2-methyl-2,4-pentanediol complex, is also shown (21).

$\Delta R_{MQ,ex}$ rates with single k_{ex} and p_E values from these methyl groups, to obtain the k_{ex} value of 3,300 ± 30 s^{-1} and the p_E value of 0.11 ± 0.0041 (Fig. 2*B*).

The methyl groups with marked exchange contributions were mapped onto the structure (Fig. 2*C*). These methyl groups were located on the βC strand (Val215), βD strand (Met223), βE strand (Leu246), βG strand (Ile270), βH strand (Val296, Val297, Ile298), βI strand (Ala312), and βL strand (Leu333). Notably, the affected regions nicely overlapped with the regions where significant structural changes occur in the gating of the cytoplasmic G-loop gate, which is responsible for the Gβγ-dependent K^+ conduction (Fig. S1 *D–G*) (19, 30), suggesting that the observed exchange processes reflect the conformational changes associated with the G-loop gating. Considering that the crystal structure of $GIRK_{CP}$ resembles the structure of the CP region with the open G-loop gate in a backbone conformation, we assumed that the ground and excited states represent the open and closed G-loop conformations, respectively. This assumption is further supported by the results of the E304A mutant (*SI Text* and Fig. S5).

Ethanol Stabilizes the Open G-Loop Conformation of $GIRK_{CP}$. To investigate whether ethanol affects the conformational exchange processes in $GIRK_{CP}$, we conducted MQ CPMG RD and methyl-HDR experiments in the presence of ethanol. Remarkably, the exchange contributions to the MQ relaxation rates significantly decreased as the concentration of ethanol increased (Fig. 3*A*). The fitting of the MQ CPMG RD curves revealed that the closed-state population decreased to 0.093 ± 0.004 in the presence 0.5 M ethanol, compared with the closed-state population of 0.110 ± 0.004 in the absence of ethanol (Fig. 3 *B* and *D*). Although it was difficult to calculate the closed-state population in the presence of 2.0 M ethanol, due to the nearly flat dispersion profiles, we estimated the closed-state population to be 0.02–0.07 based on the observed $R_{MQ,ex}$ values (3.8 s^{-1} for Ile270 and 10.2 s^{-1} for Ile298 at 14.1 tesla), assuming that the chemical shift differences are not significantly perturbed and that the k_{ex} value is within the range of 3,000–5,000 s^{-1}. These results indicate that ethanol shifts the conformational equilibrium to stabilize the open state. The stabilization of the open state was also evident from the peak positions of Ile270 and Ile298, which shifted toward the open-state peak positions as the ethanol concentration increased (Fig. 3*C*).

The TM Region Affects the Conformational Exchange Processes in the CP Region. Although the results from $GIRK_{CP}$ quantitatively explained the mechanism of the ethanol action, electrophysiological studies showed that the open probability of GIRK was as low as 0.1–0.3 in the absence of ethanol (8, 38), which is apparently inconsistent with our result that the majority of $GIRK_{CP}$ adopts the open G-loop conformation in the absence of ethanol. We assumed that this difference originated from the absence of the transmembrane segment, which could affect the conformational exchange processes in the CP region. In fact, a set of crystal structures and our previous NMR analyses revealed that the CP region is structurally coupled to the TM region, through interactions involving the G-loop residues (17, 18, 30).

To investigate the effects of the presence of the TM region on the conformational exchange processes in the CP region, we analyzed a chimeric channel of GIRK1 (GIRK chimera), in which three-fourths of the transmembrane region were replaced with the pore of prokaryotic KirBac1.3 (17) (Fig. S6 *A* and *B*). The structure of the GIRK chimera is very similar to that of the mammalian GIRK, and an electrophysiological study revealed that the GIRK chimera could be activated by the addition of ethanol in planar lipid bilayers (39). The apparent molecular weight of the tetrameric GIRK chimera is about 200,000 in

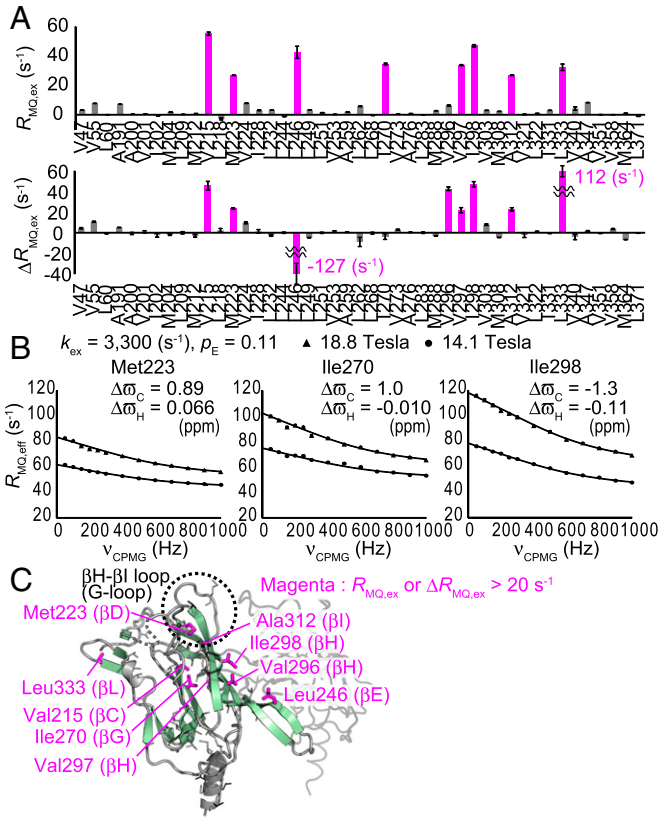

Fig. 2. MQ CPMG RD and methyl-HDR analyses of GIRK$_{CP}$ in the absence of ethanol. (*A*) Plots of $R_{MQ,ex}$ rates obtained from the MQ CPMG RD experiments and $\Delta R_{MQ,ex}$ rates obtained from the methyl-HDR experiments. The $R_{MQ,ex}$ rates at 18.8 tesla (800-MHz ^{1}H frequency) and the $\Delta R_{MQ,ex}$ rates at 14.1 tesla (600-MHz ^{1}H frequency) are shown. (*B*) Fitting curves of the MQ CPMG RD profiles measured at 14.1 tesla (600-MHz ^{1}H frequency; circles) and 18.8 tesla (800-MHz ^{1}H frequency; triangles). (*C*) Mapping of the methyl groups with exchange contributions larger than 20 s^{-1} on the structure of GIRK$_{CP}$ (PDB ID code 1N9P) (16).

detergent micelles, which is near the upper molecular weight limit for NMR analyses, so we prepared a {u-[^{2}H]; Ileδ1, Metε-[^{13}CH$_3$]} GIRK chimera sample and observed the ^{1}H–^{13}C HMQC spectra, to apply the methyl-TROSY techniques. The overlaid ^{1}H–^{13}C HMQC spectra of {u-[^{2}H]; Ileδ1, Metε-[^{13}CH$_3$]} GIRK chimera in *n*-dodecyl-β-D-maltoside micelles and {u-[^{2}H]; Ileδ1, Metε-[^{13}CH$_3$]} GIRK$_{CP}$ are shown in Fig. 4. The chemical shift differences were relatively small, and we were able to transfer the assignments of the signals from the CP region. The small chemical shift differences observed in Ile228 and Met308 are caused by the local structural differences between GIRK$_{CP}$ and the GIRK chimera. The difference in the Ile228 chemical shift reflects the difference in the ring current effect from the aromatic ring of Phe196, which is located in the TM–CP interface and adopts different conformations between the two constructs. In addition, the difference in the Met308 chemical shift is caused by the steric contacts formed between the TM helix (Fig. S6*C*). Although relaxation experiments were difficult to conduct due to the low protein concentration, we evaluated the conformational exchange processes of the GIRK chimera from the peak positions of the exchanging methyl groups. As expected, the peak positions of the Ile270 and Ile298 methyl groups, which are distant from the TM region and hence reflect the structural changes in the cytoplasmic G-loop gate, remarkably shifted toward the closed-state peak positions, supporting the hypothesis that the equilibrium shifted toward the closed state in the presence of the TM region. The shift in the peak position toward the closed state was similarly observed in Met223, which also reflects the open–closed equilibrium (Fig. 4 and Fig. S7). If we assume that the chemical shifts of the closed and open states are identical to those observed in GIRK$_{CP}$, then the open- and closed-state populations of the GIRK chimera are estimated to be about 0.40 and 0.60, respectively, from the peak positions of Ile270 and Ile298 (Fig. S8 *A*–*C*). The results obtained with the GIRK chimera are in better agreement with the electrophysiological studies in the absence of ethanol than those of GIRK$_{CP}$, in which the open state is predominantly populated (8, 38). Moreover, these observations are consistent with the crystal structure of the GIRK chimera, in which the G-loop gate was solved as a partially closed conformation (Fig. S1 *F* and *G*).

We also analyzed the changes in the NMR spectra of the GIRK chimera upon the addition of ethanol (Fig. S8*D*). The chemical shift changes observed in the GIRK chimera were very similar to those observed in GIRK$_{CP}$, indicating that ethanol binds to the GIRK chimera and shifts the conformational equilibrium to stabilize the open conformation of the G-loop gate, as in the case of GIRK$_{CP}$. From the peak positions of Ile270 and Ile298, the populations of the open state were estimated to be about 0.59 and 0.76 in the presence of 1.0 and 2.0 M ethanol, respectively. Small but significant chemical shift changes were also observed in the signals from the TM region, suggesting that the ethanol-induced changes in the CP region are allosterically coupled to the structural changes in the TM region.

Discussion

The ethanol titration experiment indicated that ethanol binds to GIRK$_{CP}$ with an apparent K_d of 1.0 M. Although the apparent K_d of 1.0 M appears to be quite large, the K_d value is consistent

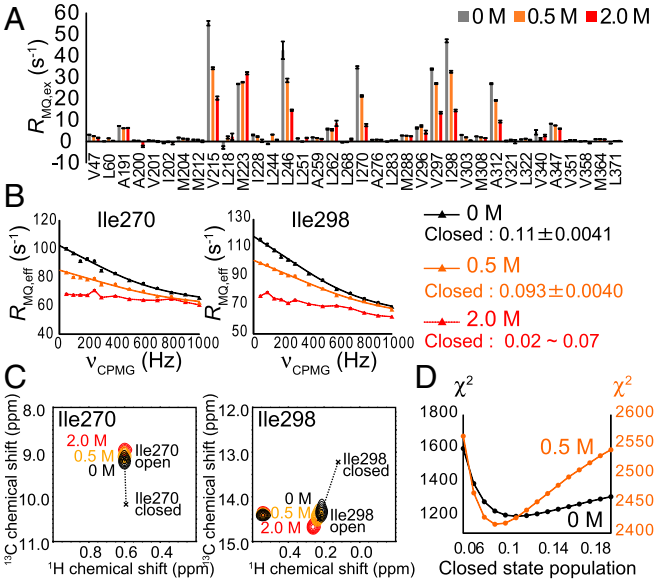

Fig. 3. Effects of ethanol on the conformational exchange processes of GIRK$_{CP}$. (*A*) Plots of $R_{MQ,ex}$ rates from MQ CPMG RD experiments in the absence (gray) and in the presence of 0.5 M (orange) and 2.0 M (red) ethanol. The $R_{MQ,ex}$ rates at 18.8 tesla (800-MHz ^{1}H frequency) are shown. (*B*) MQ CPMG RD curves in the absence (black) and in the presence of 0.5 M (orange) and 2.0 M (red) ethanol. Black and orange lines represent the fitting curves of the MQ CPMG RD profiles. (*C*) Overlay of ^{1}H–^{13}C HMQC signals of Ile270 and Ile298 in the absence (black) and in the presence of 0.5 M (orange) and 2.0 M (red) ethanol. Cross marks denote the chemical shifts of the open and closed states, which were calculated using the exchange parameters from the MQ CPMG RD and methyl-HDR analyses. (*D*) Plots of the X^2 values as a function of the closed-state population in the absence (black) and in the presence of 0.5 M ethanol (orange).

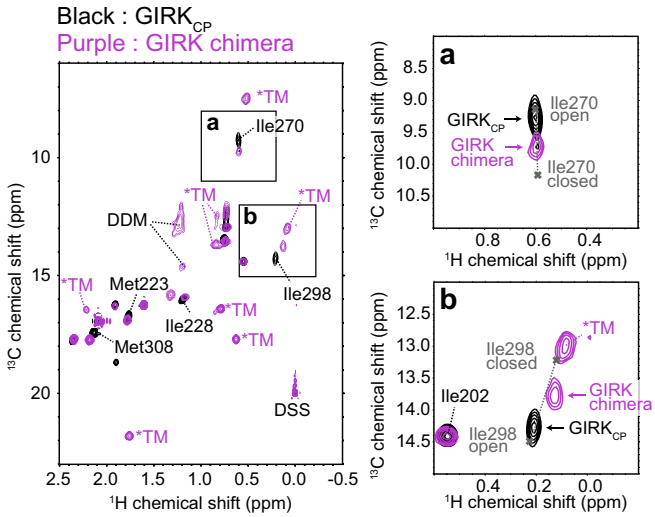

Fig. 4. NMR analyses of the GIRK chimera. Overlay of ^{1}H–^{13}C HMQC spectra of {u-[^{2}H]; Ileδ1, Metε-[^{13}CH$_3$]} GIRK$_{CP}$ (black) and {u-[^{2}H]; Ileδ1, Metε-[^{13}CH$_3$]} GIRK chimera (purple). The signals from the TM region are labeled with asterisks, and the signals with chemical shift differences are labeled. The close-up views of the ^{1}H–^{13}C HMQC signals of Ile270 (*A*) and Ile298 (*B*) are shown. Cross marks denote the chemical shifts of the open and closed states, which were calculated using the exchange parameters from the MQ CPMG RD and methyl-HDR analyses.

with the electrophysiological studies of GIRK, which showed that 200 mM ethanol did not fully activate GIRK (8, 9). Although the ethanol-bound population of GIRK is expected to be about 1.8%, assuming a blood ethanol concentration of 18 mM, which is relevant to human consumption (10), it has been proposed that a relatively small increase in the K^+ current could have a substantial effect on the membrane excitability of neurons, by lowering the equilibrium potential and drawing farther from the firing threshold (9). Furthermore, functional analyses of GIRK by Slesinger's group have suggested that the ethanol-induced activation of GIRK can be cooperatively potentiated by other activators of GIRK, such as PIP_2 and cholesterol, which are usually present in native cell membranes (15, 22). Thus, the activated fraction of GIRK under physiological conditions is expected to be higher than that calculated using the in vitro K_d value obtained from our NMR analyses. Therefore, we concluded that the K_d of 1.0 M is reasonable for the interaction between GIRK and ethanol.

The results from the MQ CPMG RD and the methyl-HDR analyses revealed that the CP region of GIRK exists in a conformational equilibrium between the open and closed conformations of the G-loop gate. The k_{ex} values and the closed-state populations were almost identical in all methyl groups except for Leu246, suggesting that the structural transitions between the states occur in a highly correlated manner. The analyses of the X^2 values as functions of the exchange parameters revealed that only Leu246 is strongly affected by a distinct exchange process, with larger k_{ex} (>4,000 s^{-1}) and higher p_E (>0.35) values than those observed in the other residues (Fig. S4). We suppose that the distinct exchange process in Leu246 reflects the conformational plasticity for adapting to multiple binding partners, such as Gβγ, since Leu246 is located adjacent to the binding site for Gβγ (βD–βE strands) (19, 30).

The results in the presence of ethanol revealed that ethanol binding shifts the conformational equilibrium to stabilize the open G-loop conformation, which would enable GIRK to permeate K^+. The methyl groups with significant exchange contributions largely overlapped with those with significant chemical shift changes (Figs. 1*D* and 2*A*), and the quantitative analyses of the exchange parameters showed that the observed chemical shift changes are mainly attributed to the shift in conformational equilibrium (Fig. 3*C*). These results indicate the dynamic activation mechanism of GIRK by ethanol, in which ethanol activates GIRK by shifting the conformational equilibrium to stabilize the G-loop gate in the open conformation, rather than by inducing static structural changes (Fig. 5).

The results of the line shape analyses and ethanol-titration experiments of the GIRK chimera indicated that the conformational exchange processes and the ethanol-induced spectral changes in GIRK$_{CP}$ were well replicated in the GIRK chimera, which closely mimics the full-length GIRK, supporting the idea that the structural and dynamic changes observed in GIRK$_{CP}$ are preserved in the presence of the TM region (Fig. S8). The marked difference between the GIRK chimera and GIRK$_{CP}$ is that the population of the closed state in the GIRK chimera (=0.60) is larger than that observed in GIRK$_{CP}$ (=0.11) in the absence of ethanol (Fig. 4). The increase in the closed-state population in the GIRK chimera is consistent with the electrophysiological results that the closed state is predominantly populated in the absence of ethanol (open probabilities of 0.1–0.3 in GIRK, and 0.19 in the GIRK chimera) (8, 38, 39). The stabilization of the closed state is probably induced by the interactions formed between the βC–βD loop and the linker connecting the CP and TM regions, since the interactions are lost in GIRK$_{CP}$. In fact, the Ala substitution of Arg201 in GIRK2, which is located on the CP–TM linker region, led to constitutive activation, and the crystal structure of the R201A mutant revealed the open G-loop gate (18). The ethanol titration results of the GIRK chimera showed that the open-state population increased from 0.40 to 0.59 and 0.76 upon the addition of 1.0 and 2.0 M ethanol, respectively (Fig. S8*D*). Although the increase in the open-state population is smaller than that obtained by the electrophysiological study of the GIRK chimera, in which the open probability increased from 0.19 to 0.54 upon the addition of 174 mM ethanol (39), the shift in the equilibrium would be sufficient for provoking the opening of GIRK. We suppose that the differences in the populations between the NMR and electrophysiological results are due to the differences in the membrane environment,

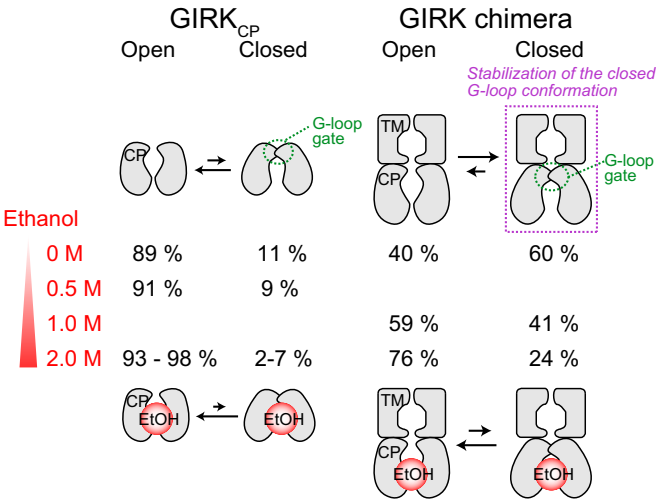

Fig. 5. Schematic representations of the conformational equilibria in GIRK$_{CP}$ and the GIRK chimera, and the effects of ethanol on the equilibria. GIRK$_{CP}$ exists in conformational equilibrium between the open and closed conformations of the G-loop gate, and ethanol shifts the conformational equilibrium to stabilize the G-loop gate in the open conformation. The populations of the two states in the absence and the presence of ethanol were calculated from the MQ CPMG RD and methyl-HDR experiments with GIRK$_{CP}$, and from the peak positions of Ile270 and Il298 in the GIRK chimera.

which strongly affects the gating behavior of GIRK (17, 39), and the cooperative activation of GIRK by the membrane PIP_2 present in the electrophysiological experiments (22).

In summary, we have demonstrated that ethanol binds to the ethanol-binding pocket of GIRK, located at the interface between the neighboring cytoplasmic regions, as in the case of the Kir2.1–MPD interaction, with an apparent K_d of 1.0 M, and ethanol binding modulates the conformational exchange processes of GIRK. Based on the MQ CPMG RD and methyl-HDR results, we proposed the dynamic activation mechanism, in which ethanol activates GIRK by shifting the conformational equilibrium to stabilize the open conformation of the G-loop gate. Considering the facts that the hydrophobic property of the ethanol-binding pocket and the dynamic nature of the ethanol action are preserved in other ethanol-binding proteins (21, 23, 24), the mechanism proposed here could provide structural insights into the mechanisms of ethanol action for various types of ethanol-sensitive signaling molecules.

Materials and Methods

$GIRK_{CP}$ and the GIRK chimera proteins were expressed in *Escherichia coli* cells and purified by chromatography on Ni-NTA resin and size exclusion chromatography. All NMR measurements were performed on Bruker Avance 500, 600, or 800 spectrometers equipped with cryogenic probes. The MQ CPMG RD and methyl-HDR measurements of $GIRK_{CP}$ were performed using the reported pulse sequences (36, 37), and the dispersion curves and the $\Delta R_{MQ,ex}$ values were simultaneously analyzed to obtain the exchange parameters ($\Delta\omega_C$, $\Delta\omega_H$, k_{ex}, and p_E). Full experimental details can be found in *SI Materials and Methods*.

ACKNOWLEDGMENTS. This work was supported in part by grants from the Japan New Energy and Industrial Technology Development Organization and the Ministry of Economy, Trade, and Industry (to I.S.); the Development of Core Technologies for Innovative Drug Development Based upon IT from Japan Agency for Medical Research and Development (to I.S.); the Ministry of Education, Culture, Sports, Science and Technology/Japan Society for the Promotion of Science KAKENHI Grants JP25121707 (to M.O.), JP16H01368 (to M.O.), JP17H03978 (to M.O.), and JP17H06097 (to I.S.); a grant from Takeda Science Foundation (to M.Y.); a grant from The Vehicle Racing Commemorative Foundation (to M.O.); and a grant from SENSHIN Medical Research Foundation (to M.O.).

1. Harris RA, Trudell JR, Mihic SJ (2008) Ethanol's molecular targets. *Sci Signal* 1:re7.
2. Howard RJ, et al. (2011) Alcohol-binding sites in distinct brain proteins: The quest for atomic level resolution. *Alcohol Clin Exp Res* 35:1561–1573.
3. Mihic SJ, et al. (1997) Sites of alcohol and volatile anaesthetic action on $GABA_A$ and glycine receptors. *Nature* 389:385–389.
4. Mascia MP, Trudell JR, Harris RA (2000) Specific binding sites for alcohols and anesthetics on ligand-gated ion channels. *Proc Natl Acad Sci USA* 97:9305–9310.
5. Beckstead MJ, Phelan R, Mihic SJ (2001) Antagonism of inhalant and volatile anesthetic enhancement of glycine receptor function. *J Biol Chem* 276:24959–24964.
6. Lovinger DM, White G, Weight FF (1989) Ethanol inhibits NMDA-activated ion current in hippocampal neurons. *Science* 243:1721–1724.
7. Wafford KA, et al. (1991) Ethanol sensitivity of the $GABA_A$ receptor expressed in *Xenopus* oocytes requires 8 amino acids contained in the γ 2L subunit. *Neuron* 7:27–33.
8. Kobayashi T, et al. (1999) Ethanol opens G-protein-activated inwardly rectifying K^+ channels. *Nat Neurosci* 2:1091–1097.
9. Lewohl JM, et al. (1999) G-protein-coupled inwardly rectifying potassium channels are targets of alcohol action. *Nat Neurosci* 2:1084–1090.
10. Bodhinathan K, Slesinger PA (2014) Alcohol modulation of G-protein-gated inwardly rectifying potassium channels: From binding to therapeutics. *Front Physiol* 5:76.
11. Bichet D, Haass FA, Jan LY (2003) Merging functional studies with structures of inward-rectifier K^+ channels. *Nat Rev Neurosci* 4:957–967.
12. Hibino H, et al. (2010) Inwardly rectifying potassium channels: Their structure, function, and physiological roles. *Physiol Rev* 90:291–366.
13. Blednov YA, Stoffel M, Chang SR, Harris RA (2001) Potassium channels as targets for ethanol: Studies of G-protein-coupled inwardly rectifying potassium channel 2 (GIRK2) null mutant mice. *J Pharmacol Exp Ther* 298:521–530.
14. Blednov YA, Stoffel M, Alva H, Harris RA (2003) A pervasive mechanism for analgesia: Activation of GIRK2 channels. *Proc Natl Acad Sci USA* 100:277–282.
15. Glaaser IW, Slesinger PA (2017) Dual activation of neuronal G protein-gated inwardly rectifying potassium (GIRK) channels by cholesterol and alcohol. *Sci Rep* 7:4592.
16. Nishida M, MacKinnon R (2002) Structural basis of inward rectification: Cytoplasmic pore of the G protein-gated inward rectifier GIRK1 at 1.8 Å resolution. *Cell* 111:957–965.
17. Nishida M, Cadene M, Chait BT, MacKinnon R (2007) Crystal structure of a Kir3.1-prokaryotic Kir channel chimera. *EMBO J* 26:4005–4015.
18. Whorton MR, MacKinnon R (2011) Crystal structure of the mammalian GIRK2 K^+ channel and gating regulation by G proteins, PIP_2, and sodium. *Cell* 147:199–208.
19. Whorton MR, MacKinnon R (2013) X-ray structure of the mammalian GIRK2-βγ G-protein complex. *Nature* 498:190–197.
20. Pegan S, Arrabit C, Slesinger PA, Choe S (2006) Andersen's syndrome mutation effects on the structure and assembly of the cytoplasmic domains of Kir2.1. *Biochemistry* 45:8599–8606.
21. Aryal P, Dvir H, Choe S, Slesinger PA (2009) A discrete alcohol pocket involved in GIRK channel activation. *Nat Neurosci* 12:988–995.
22. Bodhinathan K, Slesinger PA (2013) Molecular mechanism underlying ethanol activation of G-protein-gated inwardly rectifying potassium channels. *Proc Natl Acad Sci USA* 110:18309–18314.
23. Kruse SW, Zhao R, Smith DP, Jones DNM (2003) Structure of a specific alcohol-binding site defined by the odorant binding protein LUSH from *Drosophila melanogaster*. *Nat Struct Biol* 10:694–700.
24. Sauguet L, et al. (2013) Structural basis for potentiation by alcohols and anaesthetics in a ligand-gated ion channel. *Nat Commun* 4:1697.
25. Bucci BK, Kruse SW, Thode AB, Alvarado SM, Jones DNM (2006) Effect of *n*-alcohols on the structure and stability of the *Drosophila* odorant binding protein LUSH. *Biochemistry* 45:1693–1701.
26. Imai S, Osawa M, Takeuchi K, Shimada I (2010) Structural basis underlying the dual gate properties of KcsA. *Proc Natl Acad Sci USA* 107:6216–6221.
27. Imai S, et al. (2012) Functional equilibrium of the KcsA structure revealed by NMR. *J Biol Chem* 287:39634–39641.
28. Minato Y, et al. (2016) Conductance of $P2X_4$ purinergic receptor is determined by conformational equilibrium in the transmembrane region. *Proc Natl Acad Sci USA* 113:4741–4746.
29. Osawa M, et al. (2009) Evidence for the direct interaction of spermine with the inwardly rectifying potassium channel. *J Biol Chem* 284:26117–26126.
30. Yokogawa M, Osawa M, Takeuchi K, Mase Y, Shimada I (2011) NMR analyses of the Gβγ binding and conformational rearrangements of the cytoplasmic pore of G protein-activated inwardly rectifying potassium channel 1 (GIRK1). *J Biol Chem* 286:2215–2223.
31. Mase Y, Yokogawa M, Osawa M, Shimada I (2012) Structural basis for modulation of gating property of G protein-gated inwardly rectifying potassium ion channel (GIRK) by i/o-family G protein α subunit ($G\alpha_{i/o}$). *J Biol Chem* 287:19537–19549.
32. Yokogawa M, Muramatsu T, Takeuchi K, Osawa M, Shimada I (2009) Backbone resonance assignments for the cytoplasmic regions of G protein-activated inwardly rectifying potassium channel 1 (GIRK1). *Biomol NMR Assign* 3:125–128.
33. Tugarinov V, Hwang PM, Ollerenshaw JE, Kay LE (2003) Cross-correlated relaxation enhanced ^1H–^{13}C NMR spectroscopy of methyl groups in very high molecular weight proteins and protein complexes. *J Am Chem Soc* 125:10420–10428.
34. Kuo A, et al. (2003) Crystal structure of the potassium channel KirBac1.1 in the closed state. *Science* 300:1922–1926.
35. Enkvetchakul D, et al. (2004) Functional characterization of a prokaryotic Kir channel. *J Biol Chem* 279:47076–47080.
36. Toyama Y, Osawa M, Yokogawa M, Shimada I (2016) NMR method for characterizing microsecond-to-millisecond chemical exchanges utilizing differential multiple-quantum relaxation in high molecular weight proteins. *J Am Chem Soc* 138:2302–2311.
37. Korzhnev DM, Kloiber K, Kanelis V, Tugarinov V, Kay LE (2004) Probing slow dynamics in high molecular weight proteins by methyl-TROSY NMR spectroscopy: Application to a 723-residue enzyme. *J Am Chem Soc* 126:3964–3973.
38. Lesage F, et al. (1995) Molecular properties of neuronal G-protein-activated inwardly rectifying K^+ channels. *J Biol Chem* 270:28660–28667.
39. Leal-Pinto E, et al. (2010) Gating of a G protein-sensitive mammalian Kir3.1 prokaryotic Kir channel chimera in planar lipid bilayers. *J Biol Chem* 285:39790–39800.
40. Chen L, et al. (2002) A glutamate residue at the C terminus regulates activity of inward rectifier K^+ channels: Implication for Andersen's syndrome. *Proc Natl Acad Sci USA* 99:8430–8435.
41. Meng XY, Zhang HX, Logothetis DE, Cui M (2012) The molecular mechanism by which PIP_2 opens the intracellular G-loop gate of a Kir3.1 channel. *Biophys J* 102:2049–2059.
42. Li J, et al. (2016) Three pairs of weak interactions precisely regulate the G-loop gate of Kir2.1 channel. *Proteins* 84:1929–1937.
43. He C, et al. (2002) Identification of critical residues controlling G protein-gated inwardly rectifying K^+ channel activity through interactions with the β γ subunits of G proteins. *J Biol Chem* 277:6088–6096.
44. Kofuji P, Davidson N, Lester HA (1995) Evidence that neuronal G-protein-gated inwardly rectifying K^+ channels are activated by G β γ subunits and function as heteromultimers. *Proc Natl Acad Sci USA* 92:6542–6546.
45. Goto NK, Gardner KH, Mueller GA, Willis RC, Kay LE (1999) A robust and cost-effective method for the production of Val, Leu, Ile (δ 1) methyl-protonated ^{15}N-, ^{13}C-, ^2H-labeled proteins. *J Biomol NMR* 13:369–374.
46. Gans P, et al. (2010) Stereospecific isotopic labeling of methyl groups for NMR spectroscopic studies of high-molecular-weight proteins. *Angew Chem Int Ed Engl* 49:1958–1962.
47. Ayala I, Sounier R, Usé N, Gans P, Boisbouvier J (2009) An efficient protocol for the complete incorporation of methyl-protonated alanine in perdeuterated protein. *J Biomol NMR* 43:111–119.
48. Wang C, Palmer AG, 3rd (2002) Differential multiple quantum relaxation caused by chemical exchange outside the fast exchange limit. *J Biomol NMR* 24:263–268.
49. Skrynnikov NR, Dahlquist FW, Kay LE (2002) Reconstructing NMR spectra of "invisible" excited protein states using HSQC and HMQC experiments. *J Am Chem Soc* 124:12352–12360.